Flux-Calibration of Medium-Resolution Spectra from 300 nm to 2500 nm

Sabine Moehler[a], Andrea Modigliani[a], Wolfram Freudling[a], Noemi Giammichele[b], Alexandros Gianninas[c], Anais Gonneau[d], Wolfgang Kausch[ef], Ariane Lançon[d], Stefan Noll[e], Thomas Rauch[g], and Jakob Vinther[a]

[a]European Southern Observatory, Karl-Schwarzschild-Str. 2, D 85748 Garching, Germany;

[b]Département de Physique, Université de Montréal, CP. 6128, Succursale Centre-Ville, Montréal, QC H3C 3J7, Canada;

[c]Homer L. Dodge Department of Physics and Astronomy, University of Oklahoma, 440 W. Brooks St., Norman, OK, 73019, USA;

[d]Observatoire astronomique de Strasbourg, Université de Strasbourg, CNRS, UMR 7550, 11 rue de l'Université, F-67000 Strasbourg, France;

[e] Institut für Astro- und Teilchenphysik, Universität Innsbruck, Technikerstr. 25/8, 6020 Innsbruck, Austria;

[f] University of Vienna, Department of Astrophysics, Türkenschanzstr. 17 (Sternwarte), 1180 Vienna, Austria;

[g] Institute for Astronomy and Astrophysics, Kepler Center for Astro and Particle Physics, Eberhard Karls University, Sand 1, 72076 Tübingen, Germany

ABSTRACT

While the near-infrared wavelength regime is becoming more and more important for astrophysics there are few spectrophotometric standard star data available to flux calibrate such data. On the other hand flux calibrating high-resolution spectra is a challenge even in the optical wavelength range, because the available flux standard data are often too coarsely sampled. We describe a method to obtain reference spectra derived from stellar model atmospheres, which allow users to derive response curves from 300 nm to 2500 nm also for high-resolution spectra. We verified that they provide an appropriate description of the observed standard star spectra by checking for residuals in line cores and line overlap regions in the ratios of observed spectra to model spectra. The finally selected model spectra are then empirically corrected for remaining mismatches and photometrically calibrated using independent observations. In addition we have defined an automatic method to correct for moderate telluric absorption using telluric model spectra with very high spectral resolution, that can easily be adapted to the observed data. This procedure eliminates the need to observe telluric standard stars, as long as some knowledge on the target spectrum exists.

Keywords: Flux calibration, standard stars, telluric correction

1. INTRODUCTION

Accurate flux calibration of astronomical spectra remains a significant challenge. Spectral flux calibration requires flux calibrators with known absolute fluxes that are accessible with the same spectrograph that also takes the spectra of the science targets. With the arrival of new generations of spectrographs that cover wide wavelength ranges and produce relatively high-resolution spectra, known and well-tested spectrophotometric standard star

Send correspondence to smoehler@eso.org

catalogues[1,2] are no longer adequate for spectral flux calibration because they do not extend to the near-infrared (NIR) and/or are too coarsely sampled to permit the flux calibration of high-resolution spectra. For example, the European Southern Observatory's (ESO) X-shooter instrument[3] covers, in a single exposure, the spectral range from 300 nm to 2500 nm and operates at intermediate spectral resolution (R≈4000–17 000, depending on wavelength and slit width) with fixed échelle spectral format in three optimized arms (UVB: 300 nm–550 nm, VIS: 550 nm–1000 nm, NIR: 1000 nm–2500 nm).

In this paper we present a procedure to obtain calibrated model spectra for flux standard stars covering the wavelength range from 300 nm to 2 500 nm. These spectra are useful for deriving consistent instrumental response curves over this wide range of wavelengths with a spectral resolving power of up to 40 000 and possibly more.

In order to compute response curves for an instrument from observed spectra and model spectra, the effect of the Earth's atmosphere must be removed from the observed spectra. In Sect. 3, we describe a method for fast and efficient removal of the telluric absorption features, that is sufficiently accurate for the intended purpose of deriving response curves and can be adapted for any other instrument providing spectra of sufficient resolution between 600 nm and 2 500 nm.

We restrict this paper to the description of the general aspects of our methods. Readers interested in more details are invited to look at Ref. 4.

2. REFERENCE SPECTRA

Our approach to obtain fully calibrated model spectra was as follows. First, we selected a set of flux standard stars observable from the southern hemisphere that cover the full right ascension range, whose spectra can be modelled accurately, and for which X-shooter spectra exist (Sects. 2.1, and 2.2). We then used X-shooter observations of these stars to compute the ratio of the observed spectra to the model spectra, i.e. the instrumental response (see Sect. 2.3). If the model spectra perfectly described the spectra of all stars, response curves derived from different stars observed with the same instrumental setup should only differ by signatures imposed by the atmosphere (e.g. telluric absorption, varying atmospheric transmission). However, due to small deficiencies in the model spectra, for most of the stars such ratios show star-specific features in regions dominated by overlapping lines (see Fig. 1). To be able to identify and fit such deficiencies we observed a star that does not show any lines within the X-shooter spectral range and whose spectrum can be modelled accurately. We used the ratio between model and observations of that star together with the observed spectra of all our stars to derive corrections to their model spectra. Finally, we used the available (spectro-)photometric data for the stars to compute the absolute flux scale of the corrected model spectra (see Sect. 2.4). The result is a self-consistent new set of fully flux calibrated spectrophotometric standards for the southern hemisphere.

2.1 Sample selection

Spectral flux calibration utilizes as reference either well-calibrated observations or a spectral model of a standard star. The process of flux calibration requires computing the ratio of an observed spectrum with the model, and such a ratio is less sensitive to errors in the wavelength scale if the spectrum is smooth and featureless. The advantage of using a model is that it is noiseless, and does not include features imposed by the terrestrial atmosphere. Therefore, the ideal star to be used as a spectral flux standard has a smooth and featureless spectrum that can be accurately modelled with a minimum number of parameters. The model spectrum of a star can be used to derive the *shape* of the response curve of an instrument and can therefore be used to test and improve the model spectra of other stars. If an absolute flux calibration is intended the spectral models must be accompanied by accurate absolutely calibrated (spectro-)photometric observations at some wavelengths within the wavelength range covered by the spectrum. Unfortunately, only few available standards satisfy all criteria simultaneously, as all available flux standard stars have some features in their spectrum.

For the current work, we searched for stars with the following criteria:

1. hot white dwarfs and hot subdwarfs in order to be able to model their spectra
2. located in the southern hemisphere

3. available flux information[1,2,5]

4. available X-shooter spectra taken with a wide (5") slit to minimize slit losses

This selection resulted in six standard stars, namely EG 274, GD 71, GD 153, LTT 3218, LTT 7987 (all hot DA white dwarfs), and Feige 110 (a hot subdwarf).

For calibration purposes we then looked for a star in the southern hemisphere that has a spectrum free of absorption lines between 300 nm and 2 500 nm and found L97-3 (a DC white dwarf with a featureless spectrum in this wavelength range).

2.2 Modelling of hot white dwarfs

The spectra of our standard stars include strong hydrogen lines (in the case of Feige 110 also helium lines) that need to be properly modelled if one wants to sample the response of an instrument on scales of some nanometers.

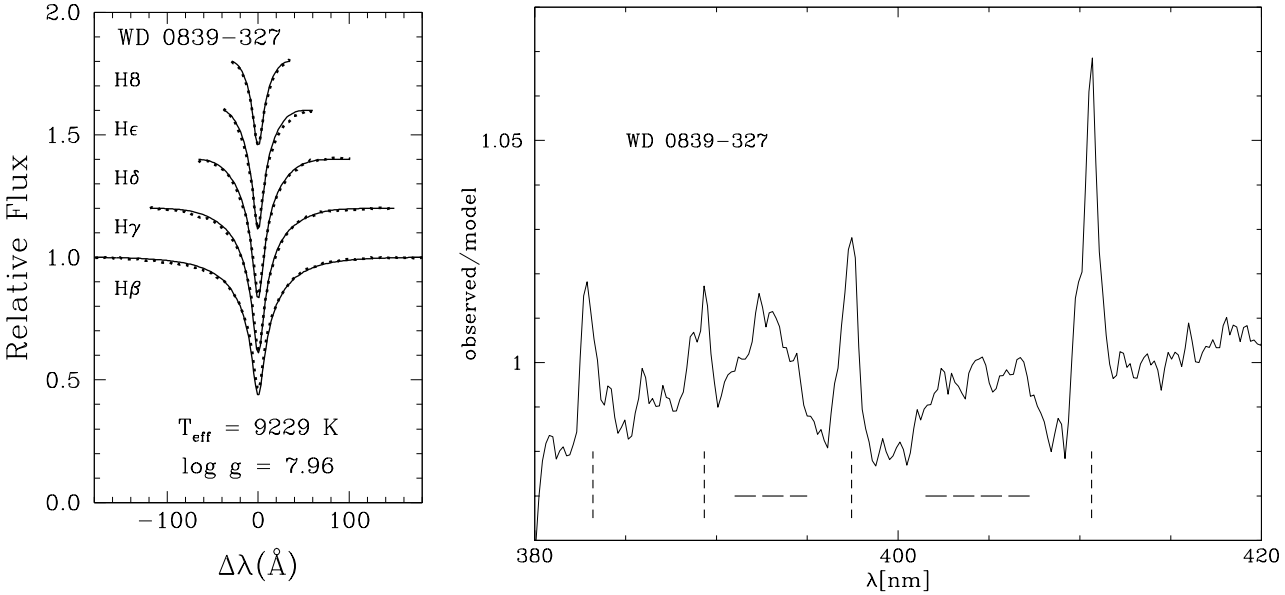

Figure 1. Model fit for LTT 3218 (individual lines only,[6] **left**, dotted/solid lines mark observed/model spectrum) and the ratio between their observation and model spectrum (**right**). The ratio plot on the right clearly shows residuals in the line cores (marked by short-dashed vertical lines) and also some bumps between the lines (marked by long-dashed horizontal lines).

For the past 20 years the physical parameters of hot white dwarfs and other hot, high-gravity stars have been determined by fitting the profiles of the hydrogen (and/or helium) absorption lines in their optical spectra[7] (see Fig. 1, left panel, for an example). This method has the advantage that it is sensitive to changes in temperature and surface gravity at high effective temperatures, when optical and near-infrared photometry become insensitive to changes in these parameters. In consequence, this means that model spectra with a wrong effective temperature or surface gravity will not correctly describe the strong hydrogen and/or helium absorption lines in the spectra of these stars. Such a mismatch is most severe at the blue end of the wavelength range studied in this paper, namely between 380 nm and 420 nm, where the lines may overlap with each other, causing a lack of continuum. An example of such a mismatch can be seen in the right panel of Fig. 1, which shows the ratio of the observed spectrum to the fitted model spectrum for LTT 3218. The bumps at 390 nm–395 nm and 400 nm–410 nm are caused by an imperfect description of the line overlap region between the Balmer lines at 389 nm (H8), 397 nm (Hϵ), and 410 nm (Hδ). Compared to the line depths of about 50% the effects are small (about 2%), but sufficient to introduce noticeable artefacts in the resulting response curves. To ensure that no such mismatches exist in

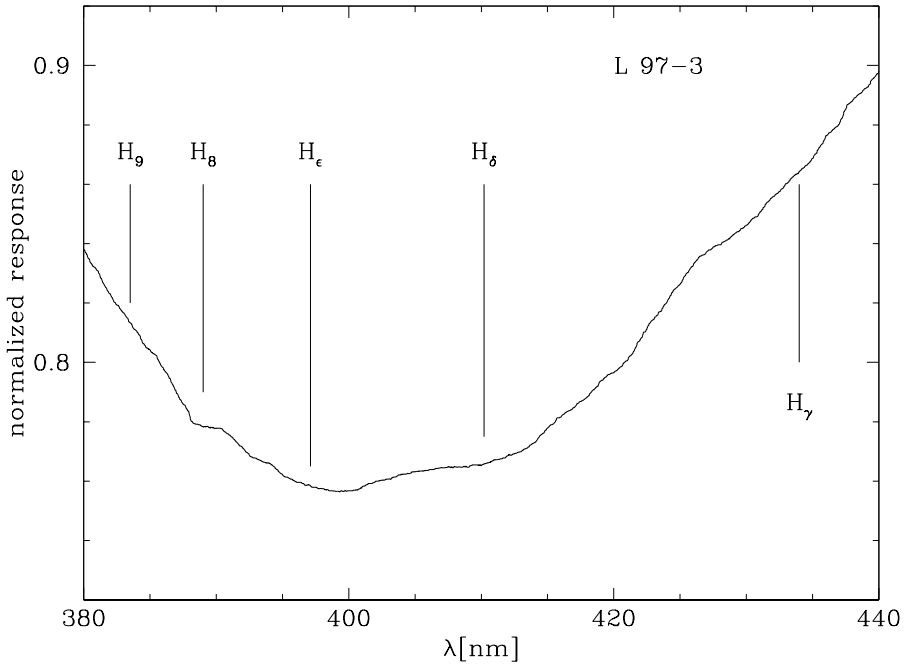

Figure 2. Average ratio of observed standard spectrum and shifted reference spectrum for L97-3 for the same wavelength ranges as in Fig. 4.

the finally selected reference spectra, however, one has to know the true response of the instrument with which the spectra, that are used for the analysis, are observed.

This was the primary motivation to include L97−3, whose featureless spectrum can easily be modelled in the wavelength range discussed here. This is illustrated in Fig. 2, which shows the ratio of model spectrum to observed spectrum for L97-3 for the regions containing strong and overlapping lines in the spectra of the flux standard stars discussed here. We used as reference data a stellar model spectrum[8] calculated for the parameters reported by Ref. 6 for this star. This model spectrum was adjusted to the published photometry of the star. The curve in Fig. 2 is rather smooth without significant structure on nanometer scales (as opposed to Fig. 1).

2.3 Selection and empirical correction of model spectra

We used X-shooter observations of the six standard stars to verify the quality of the various model spectra available for them by comparing instrumental response curves from different standard stars. We concentrated first on the wavelength range 380 nm to 440 nm for the reasons discussed above. Once an acceptable description of the blue range has been achieved we verified its suitability for the redder wavelength ranges as well. For our analysis we used one-dimensional extracted and merged X-shooter spectra of the flux standard stars processed with the reflex workflow[9] (http://www.eso.org/sci/software/pipelines/) of X-shooter. These spectra were then corrected for atmospheric extinction using the Paranal extinction curve[4,10] and normalized by exposure time.

We aligned the model spectrum for a given star to the same radial velocity as the observed spectrum to avoid the introduction of pseudo-P Cygni profiles when the observed spectrum is divided by the model spectrum. Each observed standard star spectrum was divided by the shifted reference star spectrum. Finally the ratios were averaged per star to achieve a better signal-to-noise ratio. This provided us with raw, i.e. unsmoothed, response curves that allowed us to look for systematic discrepancies between the observed and the model spectra. Any feature in these ratios that does not appear for all standard stars points strongly towards deficiencies in the reference spectra as instrumental effects should not depend on which standard star is used. We selected as best description of the UVB spectrum those model spectra that showed the smallest star-specific bumps in the averaged ratio spectra.

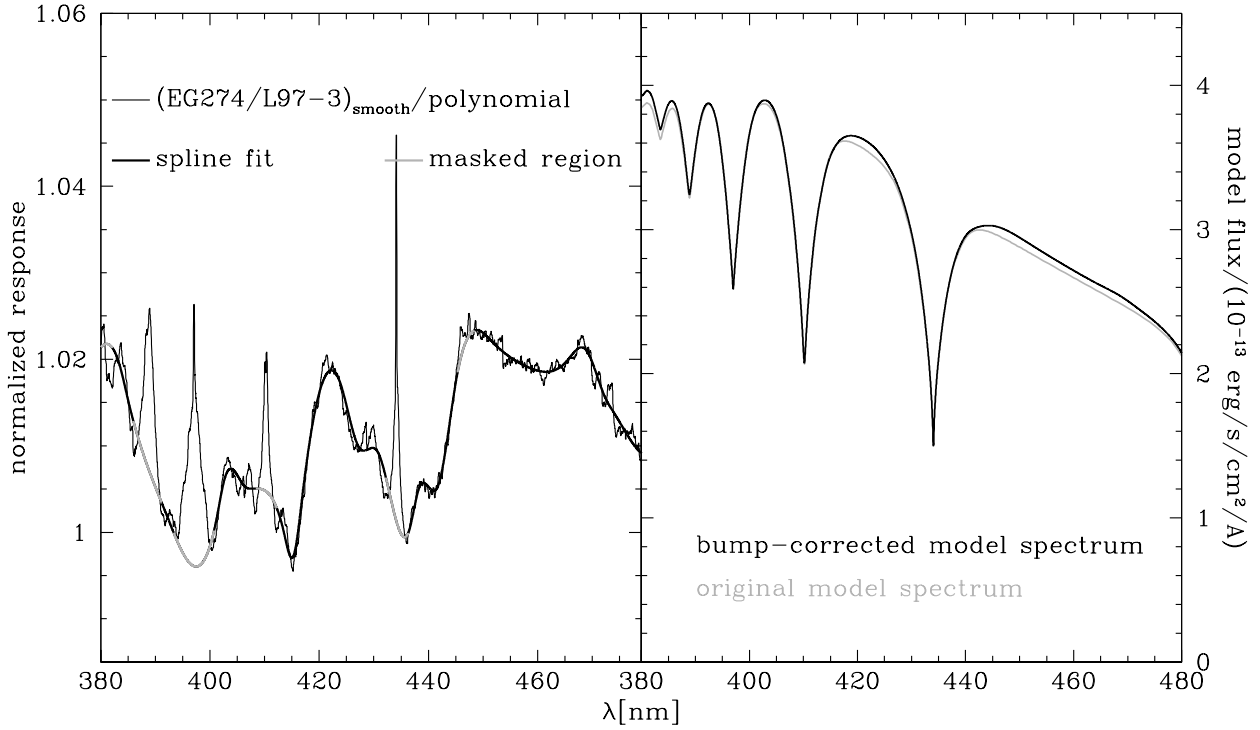

Figure 3. **Left:** Ratio of average raw response for EG 274 and smoothed response for L97-3, normalized by a low-order polynomial to remove large scale variations, and smoothed (thin black line). The narrow spikes are due to mismatches in the line cores, while the broad bumps at 405 nm, 420 nm, and 460 nm are due to imperfect line broadening, which underestimates the flux between the lines in the model spectra. The thin black curve was fit with a spline (thick black line) after masking the regions of the line cores (masked regions in grey). **Right:** Model spectrum before correction (grey) and corrected with the fit (black).

In order to correct the remaining mismatches between observed and model spectra that cause bumps like those seen in Fig. 1 we divided the average raw response of each star by the smoothed response curve derived from L97-3. The products of this procedure are expected to be equal to 1 in an ideal case, but differences in atmospheric conditions result in residual slopes. Remaining mismatches between model spectra and observations cause narrow spikes and bumps that we want to correct (see Fig. 3, left). For every star we fitted the shape of this ratio spectrum by a low-order polynomial fit to remove the large-scale variations. Then we smoothed the result and fit the remaining bumpy regions (see Fig. 3, left, for an example). Applying the fit to the model spectrum we obtained the black curve shown in Fig. 3 (right).

The bump corrections were smallest for GD 71, GD 153, and Feige 110, while EG 274, LTT 7987, and LTT 3218 had significant corrections (increasing in this order). This is expected as the last three stars have the strongest and widest lines and thus present the biggest challenge when it comes to the correct treatment of overlapping lines. Since the mismatches in the line cores were not corrected (as they vary with spectral resolution) some masking is still required when fitting a response (see Sect. 2.5). We also verified that in the spectral range 450 nm to 2 500 nm the only residuals seen in the response curves are those in the line cores of hydrogen and/or helium lines.

2.4 Absolute flux calibration

We have now defined a set of model spectra which adequately reproduce the observed X-shooter spectra of the six flux standard stars, with residuals (outside line cores, that are affected by resolution effects) well below 2%. To allow a proper flux calibration we have to verify that the overall flux distribution of these model spectra reproduces the independently observed (spectro-)photometric data. To do so we convolved the model spectra

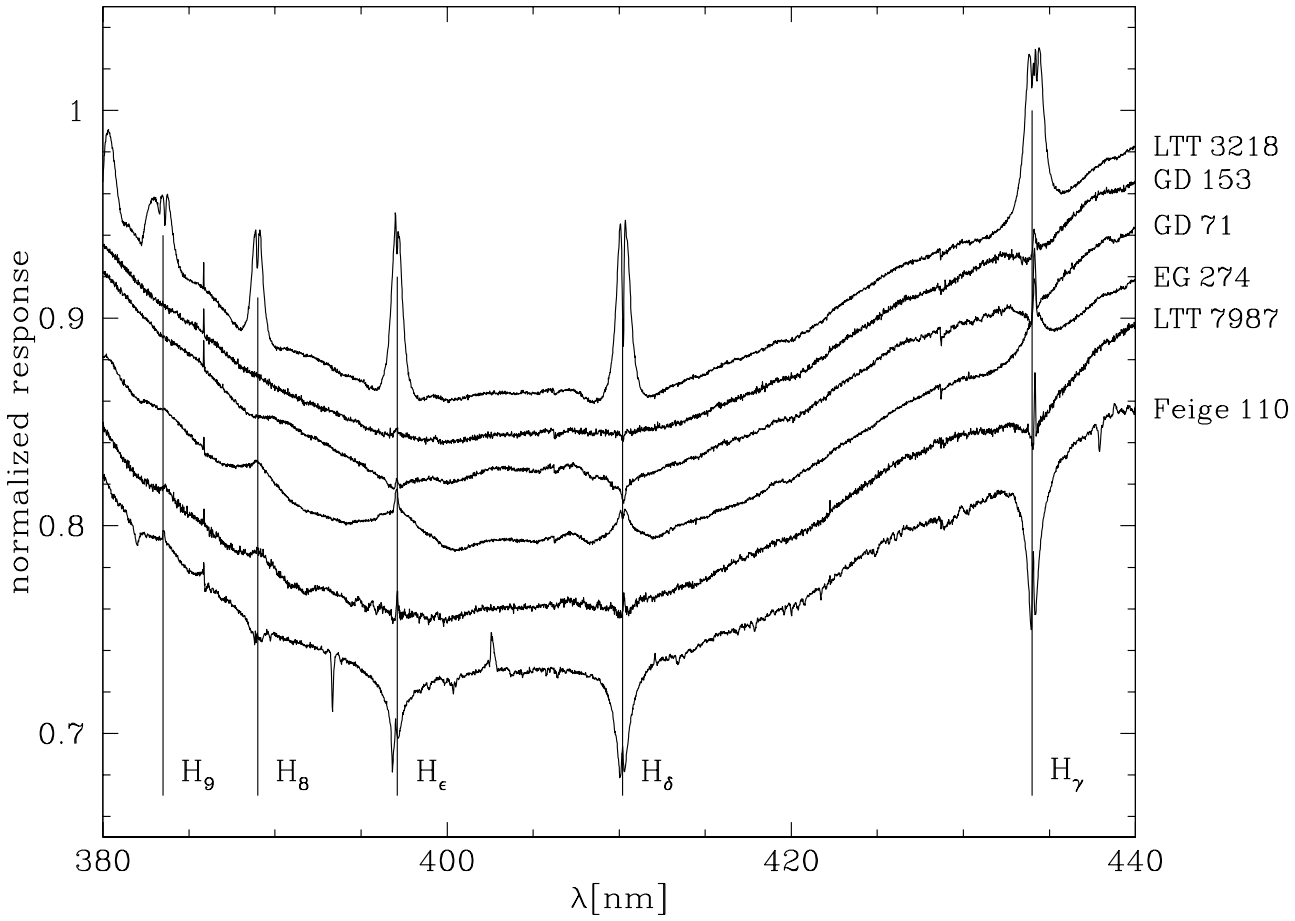

Figure 4. Average ratios of observed standard star spectrum (corrected for atmospheric extinction) and shifted reference spectrum using the bump-corrected model spectra. The curves have been normalized at the 450 nm and were offset in steps of 0.02 for better visibility. The positions of the Balmer lines are marked. Feige 110 in addition has helium lines and interstellar Ca II lines in its spectrum.

to a resolution of 1.6 nm for the UVB/VIS spectral range and then binned them to 5 nm steps to reproduce the tabulated data.[1,2] For the NIR range we convolved the data to a resolving power of 2000 (J band) and 1500 ($H+K$ band) and integrated them over the wavelength ranges given in Ref. 11 for EG 274, Feige 110, LTT 3218, and LTT 7987. These flux values were then converted to pseudo-magnitudes

$$mag = -2.5 \cdot \log(flux) \tag{1}$$

and aligned to the respective (spectro-)photometric data by a constant factor across the full wavelength range. For GD 71 and GD 153 our new model spectra could also be aligned by a constant factor to the HST model spectra.[5] Figure 4 shows the average ratio of observed and reference spectra for the new model spectra.

2.5 Fitting of the response

The ratio of the observed spectrum to the shifted reference spectrum usually shows residuals at the line cores. At the same time the ratio spectra may show variations on intermediate scales that need to be fit by the response curve because they are instrumental features. Therefore one has to decide which regions should be avoided during the fit. We found the best solution for this problem to be with a list of fit points per star, where the median of the raw response across a pre-defined window is determined at each point. The response is then derived via a spline fit to these pre-defined points. This window increases towards longer wavelengths (from ±0.04 nm below

550 nm to ±5 nm above 1 μm) to achieve comparable signal across the full wavelength range for the hot stars studied here (see Fig. 5 for an example).

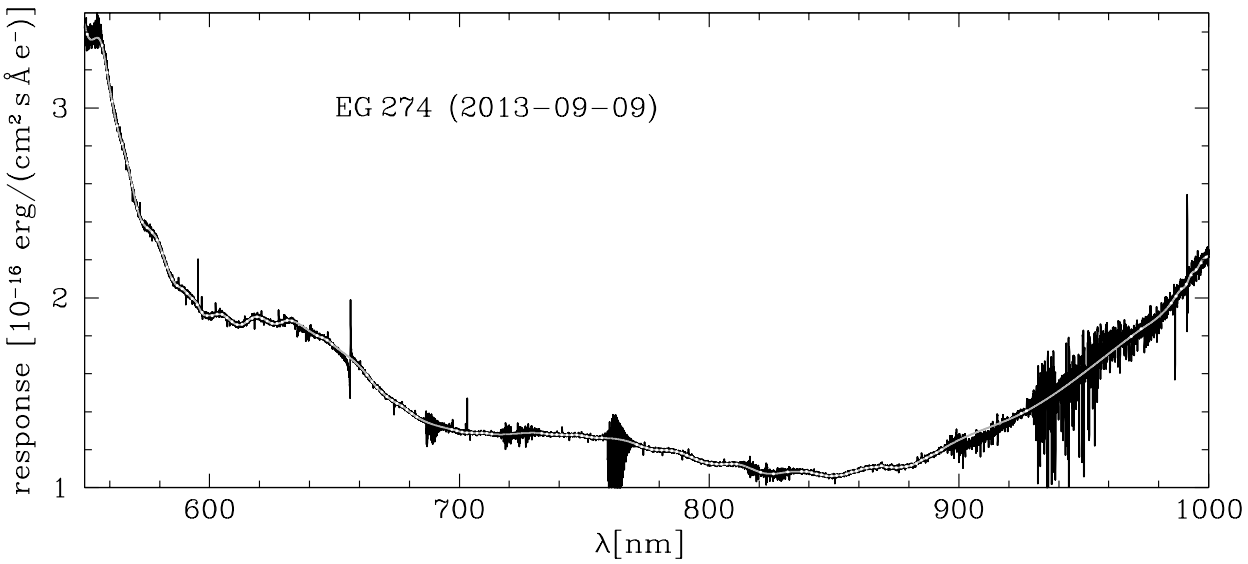

Figure 5. X-shooter response curve derived for EG 274 (VIS arm). The white dots mark the fit points described in Sect. 2.5 and the grey line marks the fit through these points.

3. CORRECTION OF ATMOSPHERIC EFFECTS

We have now defined reference spectra that describe the flux standard stars very well. In order to derive a response curve the effects of the Earth's atmosphere have to be removed from the observed spectra. Otherwise the response curve will contain a mixture of instrumental effects and atmospheric effects. The atmospheric effects consist of two major parts: atmospheric extinction (small variation with time in the case of Paranal due to the low aerosol content, which governs the extinction variability) and telluric absorption lines (strong variation with time in the case of water vapour). The first affects principally the wavelength range 300 nm to 1 000 nm and is described by the Paranal extinction curve.[4,10] The second is important for data above 600 nm.

3.1 Telluric absorption

If one does not correct at least those parts of the spectrum that contain low to medium telluric absorption, one has to interpolate the response across very wide wavelength ranges, which results in large systematic uncertainties for the resulting flux calibration. Traditionally such corrections use so-called telluric standard stars, i.e. stars with either no features or extremely well-known features in the regions of telluric absorption, that allow the user to determine the telluric absorption spectrum. This method relies on the assumption that the conditions governing the telluric absorption have not changed between the observation of the science target and the observation of the standard star. Since this assumption is often not fulfilled, we decided instead to use a catalogue of telluric model spectra[12,13] to correct the telluric absorption lines. Alternatively, a large number of telluric standard star observations can be used to extract the principal components of the telluric transmission.[14]

The high-resolution transmission spectra ($R = 60\,000$) were calculated for the wavelength range from 300 nm to 30 μm using the LBLRTM radiative transfer code,[15] the HITRAN molecular line database,[16] and different average atmospheric profiles (pressure, temperature, and molecular abundances) for Cerro Paranal.

To identify the best telluric model spectrum to correct a given observation, the telluric model spectra first have to be aligned to the observed spectrum in both resolution and wavelength. Then the telluric model spectrum that leaves the smallest residuals after applying it to the observation has to be identified. We used the following step-by-step procedure:

1. Convert the wavelength scale (in nm) of the model and observed spectra to natural logarithm. This was done because X-shooter has a constant resolving power. For instruments with a constant FWHM the procedure described below should be done in linear wavelength space.
2. Extract appropriate ranges for cross correlation (NIR: $7.0 \leq \ln \lambda_{\rm nm} \leq 7.1$, H_2O feature; VIS: $6.828 \leq \ln \lambda_{\rm nm} \leq 6.894$, H_2O feature).
3. Cross correlate the extracted telluric model and observed spectra with a maximum shift of 500 sampling units (each of size 10^{-5}) in natural logarithmic space.
4. Fit a Gaussian profile within ± 0.001 in $\ln(\lambda)$ around the cross correlation peak.
5. Shift the logarithmic model wavelength scale by the fitted peak position of the cross-correlation curve.
6. Create a Gaussian with the measured FWHM.
7. Convolve the model spectrum with the Gaussian in $\ln(\lambda)$ space. Since the resolution of the observed spectra is about a factor of 10 lower than the resolution of the telluric model spectra, we assume here the resolution of the model spectra to be infinite.
8. Convert the shifted and convolved model spectrum to linear wavelength space.
9. Divide the observed spectrum by the convolved and shifted telluric model spectrum (whereby we avoid resampling the observed spectrum).
10. Use predefined continuum points (avoiding regions of strong telluric absorption as well as known lines of the observed star, see Sect. 2.5) to fit a cubic spline to the telluric-corrected observed spectrum.
11. Divide the telluric-corrected observed spectrum by the fit of the continuum.
12. Determine mean and rms for regions of moderate telluric absorption in the normalized corrected spectrum.

Then, we choose as best fitting model spectrum the one for which the average residuals computed over regions of moderate telluric absorption is minimal. The telluric corrected spectrum of the flux standard star is then compared to the stellar model spectrum (see Sect. 2 for details) to determine the response. Figure 6 shows examples for a good telluric correction (right) and for undercorrection (left).

The absorption in the wavelength regions 1985 nm–2030 nm and 2037 nm–2089 nm is caused mainly by CO_2 features, whose abundance is not varied in the telluric model spectra for a given airmass. These regions were therefore ignored when looking for the best fit. We did not restrict the search for the best telluric model spectrum in airmass, as we found that in some cases a telluric model spectrum for an airmass quite different from the observed one can still provide a good fit in the regions that we analyse.

Users who want to employ the telluric model spectra to correct their data can find information about the Cerro Paranal sky model[12] at http://www.eso.org/sci/software/pipelines/skytools/ together with the following pre-calculated libraries*:

1. PWV†-dependent library with 45 spectra at airmasses 1.0, 1.5, 2.0, 2.5, 3.0, and PWV (in mm) of 0.5, 1.0, 1.5, 2.5, 3.5, 5.0, 7.5, 10.0, and 20.0.
2. Time-dependent library with 35 spectra at airmasses 1.0, 1.5, 2.0, 2.5, 3.0, and bi-monthly average PWV values (1=December/January ... 6=October/November) as well as a yearly average PWV content (labelled 0). Compared to the time-dependent library used by Ref. 4 the airmass coverage has been increased, the night-time periods have been dropped, and the CO_2 content has been updated.

*ftp://ftp.eso.org/pub/dfs/pipelines/skytools/telluric_libs
†Precipitable Water Vapour

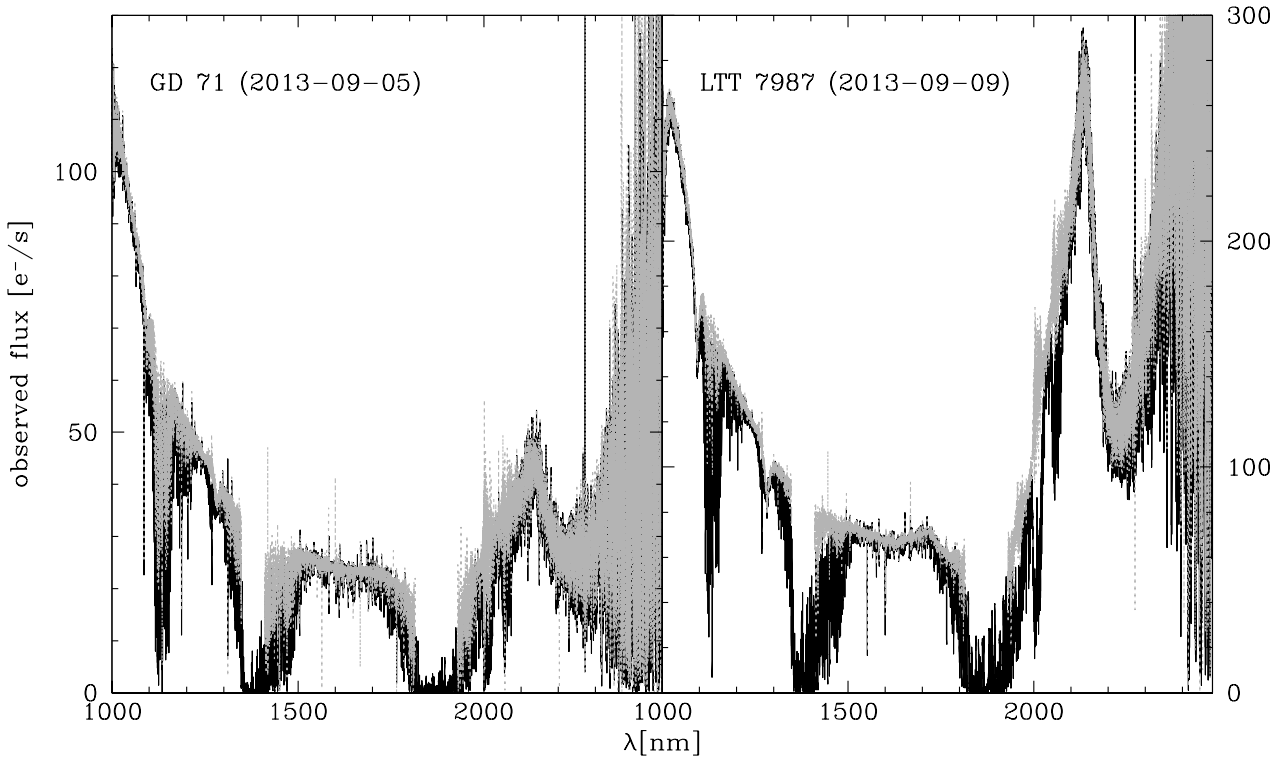

Figure 6. Results of the telluric correction (grey) for a bad (**left**) and a good (**right**) case. Regions of extremely high telluric absorption have extremely high noise in the corrected data and are therefore omitted (1348 nm–1410 nm, 1815 nm–1930 nm). The lines at 1093.5 nm and 1281.4 nm are stellar lines and the variable peak at about 2100 nm is caused by variations in the flux level and spectral energy distribution of the NIR flat field lamp.

The spectra are provided with resolutions of 60 000 and 300 000 and do not include Rayleigh scattering. The SkyCalc web application[‡] can always be used to produce sky radiance and transmission spectra with more specific parameters, including Rayleigh scattering.

The quality of the telluric correction has to be kept in mind when fitting a response to the ratio of such a corrected spectrum to the corresponding stellar model spectrum, as regions with remaining absorption or overcorrected features may distort the fit. For this reason we finally decided to mask the following regions when fitting a response curve to avoid potential telluric residuals: 634 nm–642 nm, 684 nm–696 nm, 714.7 nm–732.3 nm, 757.5 nm–770.5 nm, 813 nm–836.5 nm, 893.9 nm–924 nm, 928 nm–983 nm, 1081 nm–1171 nm, 1267 nm–1271 nm, 1300 nm–1503 nm, 1735 nm–1981 nm, 1995 nm–2035 nm, 2048 nm–2082 nm. We note that this masking rejects far less of the spectrum than would be necessary if no telluric correction had been applied.

4. SUMMARY

In this paper we have presented flux-calibrated model spectra of southern sky spectral photometric standards in the wavelength range from 300 nm to 2500 nm. The calibrated model spectra are available at the CDS. The consistency of the set of models were verified using X-Shooter observations, and the region of strong line overlap in the model spectra was adjusted taking advantage of X-shooter observations of the featureless spectrum of L97–3. Our analysis shows that the use of stellar model spectra as reference data for flux standard has significant advantages when it comes to calibrating medium-resolution data as they are available on a finely sampled wavelength grid. Another strong advantage is the fact that model spectra are not affected by telluric absorption.

Our model spectra are useful to determine the response curve of spectrographs, and the resulting response curve can in turn be used to flux-calibrate spectra of other targets. We have discussed in detail a methodology

[‡]http://www.eso.org/observing/etc/skycalc/skycalc.htm

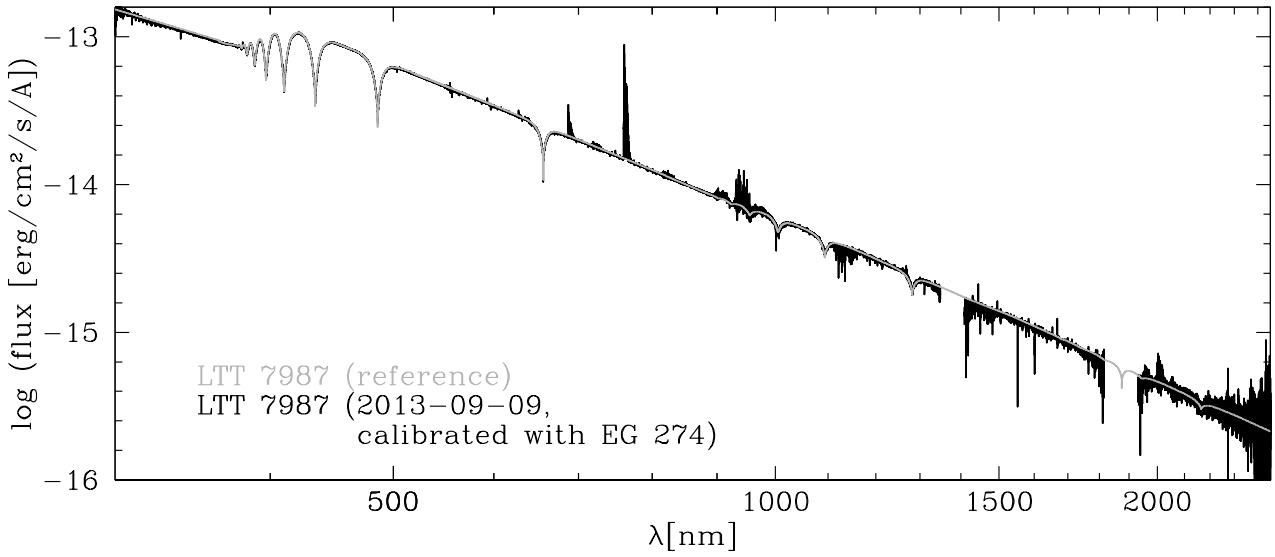

Figure 7. Spectrum of LTT 7987, corrected for telluric absorption and flux-calibrated with a response curve derived from observations of EG 274. The gray curve is the reference spectrum for LTT 7987. Regions of very high telluric absorption are omitted (1348 nm–1410 nm, 1815 nm–1930 nm).

to carry out such a flux calibration. Beyond the proper choice of stellar model spectra, an appropriate correction of telluric absorption features is essential to flux calibrate data with wavelengths above 600 nm. Our method includes the use of telluric model spectra to correct spectral regions with low to moderate telluric absorption.

To illustrate the quality that can be achieved with the methods and model spectra described in this paper, we show in Fig. 7 an example of a standard star (LTT 7987). The spectrum was flux-calibrated with the response curve determined from a different star observed on the same night, namely EG 274. Part of the response curve used for this calibration is shown in Fig. 5.

While our set of standard stars is adequate to flux calibrate spectra in the whole southern hemisphere, additional standards would be useful both to enlarge the number of potential calibrators in the south, and to provide a similar set of standards in the northern hemisphere. Our methodology can be used to derive such a set of model spectra. Necessary ingredients for such an endeavour are accurate model spectra[§], availability of flux information, and observed uncalibrated spectra for both the new calibrators and at least one of the standard stars discussed here to correct for instrumental features.

ACKNOWLEDGMENTS

This research has made use of NASA's Astrophysics Data System Bibliographic Services and of the SIMBAD database, operated at CDS, Strasbourg, France. It has been partly carried out in the framework of the Austrian ESO In-kind project funded by the Austrian Federal Ministry for Science and Research BM:wf under contracts BMWF-10.490/0009- II/10/2009 and BMWF-10.490/0008-II/3/2011 and also by the project IS538003 (Hochschulraumstrukturmittel) provided by the Austrian Ministry for Research (bmwfw). We thank D. Koester for making his model spectra available to us. We are grateful to J. Vernet, V. Mainieri, and F. Kerber for sharing their SINFONI results with us. We thank F. Patat, R. Lallement and W. Reis for their help with the improvements of the X-shooter response. TR is supported by the German Aerospace Center (DLR, grant 05 OR 1301.)

[§]For hot (pre-) white dwarfs like the flux standard stars discussed here and many others, a good starting point for model spectra would be the TMAP spectral energy distributions at the registered VO service TheoSSA (http://dc.g-vo.org/theossa) provided by the German Astrophysical Virtual Observatory (http://www.g-vo.org).

REFERENCES

[1] Hamuy, M., Walker, A. R., Suntzeff, N. B., Gigoux, P., Heathcote, S. R., and Phillips, M. M., "Southern spectrophotometric standards.," *PASP* **104**, 533–552 (July 1992).

[2] Hamuy, M., Suntzeff, N. B., Heathcote, S. R., Walker, A. R., Gigoux, P., and Phillips, M. M., "Southern spectrophotometric standards, 2," *PASP* **106**, 566–589 (June 1994).

[3] Vernet, J., Dekker, H., D'Odorico, S., Kaper, L., Kjaergaard, P., Hammer, F., Randich, S., Zerbi, F., Groot, P. J., Hjorth, J., Guinouard, I., Navarro, R., Adolfse, T., Albers, P. W., Amans, J.-P., Andersen, J. J., Andersen, M. I., Binetruy, P., Bristow, P., Castillo, R., Chemla, F., Christensen, L., Conconi, P., Conzelmann, R., Dam, J., de Caprio, V., de Ugarte Postigo, A., Delabre, B., di Marcantonio, P., Downing, M., Elswijk, E., Finger, G., Fischer, G., Flores, H., François, P., Goldoni, P., Guglielmi, L., Haigron, R., Hanenburg, H., Hendriks, I., Horrobin, M., Horville, D., Jessen, N. C., Kerber, F., Kern, L., Kiekebusch, M., Kleszcz, P., Klougart, J., Kragt, J., Larsen, H. H., Lizon, J.-L., Lucuix, C., Mainieri, V., Manuputy, R., Martayan, C., Mason, E., Mazzoleni, R., Michaelsen, N., Modigliani, A., Moehler, S., Møller, P., Norup Sørensen, A., Nørregaard, P., Péroux, C., Patat, F., Pena, E., Pragt, J., Reinero, C., Rigal, F., Riva, M., Roelfsema, R., Royer, F., Sacco, G., Santin, P., Schoenmaker, T., Spano, P., Sweers, E., Ter Horst, R., Tintori, M., Tromp, N., van Dael, P., van der Vliet, H., Venema, L., Vidali, M., Vinther, J., Vola, P., Winters, R., Wistisen, D., Wulterkens, G., and Zacchei, A., "X-shooter, the new wide band intermediate resolution spectrograph at the ESO Very Large Telescope," *A&A* **536**, A105 (Dec. 2011).

[4] Moehler, S., Modigliani, A., Freudling, W., Giammichele, N., Gianninas, A., Gonneau, A., Kausch, W., Lançon, A., Noll, S., Rauch, T., and Vinther, J., "Flux calibration of medium-resolution spectra from 300 nm to 2500 nm," *A&A* , in press (2014).

[5] Bohlin, R. C., Dickinson, M. E., and Calzetti, D., "Spectrophotometric Standards from the Far-Ultraviolet to the Near-Infrared: STIS and NICMOS Fluxes," *AJ* **122**, 2118–2128 (Oct. 2001).

[6] Giammichele, N., Bergeron, P., and Dufour, P., "Know Your Neighborhood: A Detailed Model Atmosphere Analysis of Nearby White Dwarfs," *ApJS* **199**, 29 (Apr. 2012).

[7] Bergeron, P., Saffer, R. A., and Liebert, J., "A spectroscopic determination of the mass distribution of DA white dwarfs," *ApJ* **394**, 228–247 (July 1992).

[8] Koester, D., "White dwarf spectra and atmosphere models .," *MemSAI* **81**, 921 (2010).

[9] Freudling, W., Romaniello, M., Bramich, D. M., Ballester, P., Forchi, V., García-Dabló, C. E., Moehler, S., and Neeser, M. J., "Automated data reduction workflows for astronomy. The ESO Reflex environment," *A&A* **559**, A96 (Nov. 2013).

[10] Patat, F., Moehler, S., O'Brien, K., Pompei, E., Bensby, T., Carraro, G., de Ugarte Postigo, A., Fox, A., Gavignaud, I., James, G., Korhonen, H., Ledoux, C., Randall, S., Sana, H., Smoker, J., Stefl, S., and Szeifert, T., "Optical atmospheric extinction over Cerro Paranal," *A&A* **527**, A91 (Mar. 2011).

[11] Vernet, J., Kerber, F., Saitta, F., Mainieri, V., D'Odorico, S., Lidman, C., Mason, E., Bohlin, R. C., Rauch, T., Ivanov, V. D., Smette, A., Walsh, J. R., Fosbury, R. A. E., Goldoni, P., Groot, P., Hammer, F., Horrobin, M., Kaper, L., Kjaergaard-Rasmussen, P., Pallavicini, R., and Royer, F., "Building up a database of spectro-photometric standard stars from the UV to the near-IR: a status report," in [*Society of Photo-Optical Instrumentation Engineers (SPIE) Conference Series*], *Society of Photo-Optical Instrumentation Engineers (SPIE) Conference Series* **7016**, 46 (July 2008).

[12] Noll, S., Kausch, W., Barden, M., Jones, A. M., Szyszka, C., Kimeswenger, S., and Vinther, J., "An atmospheric radiation model for Cerro Paranal. I. The optical spectral range," *A&A* **543**, A92 (July 2012).

[13] Jones, A., Noll, S., Kausch, W., Szyszka, C., and Kimeswenger, S., "An advanced scattered moonlight model for Cerro Paranal," *A&A* **560**, A91 (Dec. 2013).

[14] Chen, Y.-P., Trager, S. C., Peletier, R. F., Lançon, A., Vazdekis, A., Prugniel, P., Silva, D. R., and Gonneau, A., "The X-Shooter Spectral Library (XSL) – I. DR1. Near-UV–Optical Spectra from the First Year of the Survey," *ArXiv e-prints* (Mar. 2014).

[15] Clough, S. A., Shephard, M. W., Mlawer, E. J., Delamere, J. S., Iacono, M. J., Cady-Pereira, K., Boukabara, S., and Brown, P. D., "Atmospheric radiative transfer modeling: a summary of the AER codes," *JQRST* **91**, 233–244 (Mar. 2005).

[16] Rothman, L. S., Gordon, I. E., Barbe, A., Benner, D. C., Bernath, P. F., Birk, M., Boudon, V., Brown, L. R., Campargue, A., Champion, J.-P., Chance, K., Coudert, L. H., Dana, V., Devi, V. M., Fally, S., Flaud, J.-M., Gamache, R. R., Goldman, A., Jacquemart, D., Kleiner, I., Lacome, N., Lafferty, W. J., Mandin, J.-Y., Massie, S. T., Mikhailenko, S. N., Miller, C. E., Moazzen-Ahmadi, N., Naumenko, O. V., Nikitin, A. V., Orphal, J., Perevalov, V. I., Perrin, A., Predoi-Cross, A., Rinsland, C. P., Rotger, M., Šimečková, M., Smith, M. A. H., Sung, K., Tashkun, S. A., Tennyson, J., Toth, R. A., Vandaele, A. C., and Vander Auwera, J., "The HITRAN 2008 molecular spectroscopic database," *JQSRT* **110**, 533–572 (June 2009).